Operational domain for the new 3MW/1000s ECRH System on WEST

T. Fonghetti, R. Dumont, G. Giruzzi, J.-F. Artaud, J.-M. Bernard, F. Bouquey, C. Bourdelle, L. Delpech, J. Hillairet, P. Maget, P. Manas, P. Mollard, J. Morales, V. Ostuni, B. Robinet, and the WEST team

CEA, IRFM, F-13108 Saint-Paul-lez-Durance, France.

Abstract. The ECRH system formerly used in Tore Supra is being upgraded to start on WEST in 2023, at a power level of 1MW and frequency of 105 GHz. Its ultimate 3MW/1000s capability is expected to enlarge the WEST operational domain by increasing margins with respect to H-mode access, and by providing additional flexibility in terms of achievable scenarios using impurity and/or MHD control. This flexibility is made possible using an antenna based on three steerable mirrors for controlled power injection. In order to determine an appropriate range of EC wave injection angles for WEST scenarios, the fast and reliable ray-tracing code REMA has been interfaced with the WEST IMAS database. This allows the EC power damping rate to be quickly assessed, as well as deposition profiles to be predicted in realistic plasma conditions. Based on a typical WEST discharge at central magnetic field $B_0 \sim 3.6$ T, central line-averaged electron density $n_l \sim 4 \times 10^{19}$ m^{-3} and central electron temperature $T_{e0} \sim 3$keV, ray-tracing calculations have been performed. Comprehensive poloidal and toroidal angle scans, as well as variations of B_t, n_l and T_{e0} with respect to the reference parameters have allowed an adequate range of injection angles to be determined for efficient use of ECRH and/or ECCD in typical WEST scenarios, and compared with the mechanical limits set by the antenna mechanical characteristics. In order to further characterize the effect of this new power source in WEST scenarios, EC wave deposition and current profiles from ray-tracing calculations have been included in integrated simulation codes. It has been shown that this additional power source could allow central electron heating to be achieved, potentially alleviating the issue of radiative collapse caused by impurities observed in some situations.

1 Introduction

Radiofrequency heating systems are widely used in magnetically confined fusion devices. Three of them have been used simultaneously in Tore Supra [1]: Lower-Hybrid (LH), Ion Cyclotron Resonance Heating (ICRH) and Electron Cyclotron Resonance Heating (ECRH). In the upgrade to the WEST configuration [2], the 118 GHz ECRH system has been discontinued because its characteristics were not consistent with the new design of the machine. As a result, the former gyrotrons will be replaced by 105GHz/1MW/1000s gyrotrons to suit the new WEST geometry and power requirements. This modification also includes an upgrade of most of the EC components as a result.

The new ECRH project has been started in 2021. The EC power is expected to be available in WEST starting in 2023 with a limited power (1MW) to reach its full 3MW/1000s capability in a staged approach [3]. From a plasma scenario standpoint, this additional power source is predicted to improve access to H-Mode. In addition, it is expected that the flexibility and localization of the EC wave absorption in the plasma will be useful in the context of impurity and MHD control.

Various numerical code developments have been carried out in order to provide support to the use of ECRH power on WEST and to prepare its implementation. Firstly, the ray-tracing REMA code [4] has been interfaced with the IMAS WEST database, in order to allow simulations using plasma parameters from existing shots to be readily performed. The operational domain in terms of injection angles for the EC antenna has been established as a result. Following this development, further simulations have been made possible. The potential role of the EC power to prevent radiative collapse due to core tungsten impurity accumulation, investigated, e.g., in ASDEX Upgrade, where ECRH has been demonstrated to be an efficient method to flatten tungsten density profiles [5], has been analysed in the context of integrated modelling. Experimental data from shot 55025, featuring a radiative collapse, has been used in simulations using the RAPTOR code [6]. By comparing the LH and EC power depositions, the expected advantages provided by the new ECRH system have been assessed.

2 Improvements of the REMA ray-tracing code

The ray-tracing code REMA [4] allows electron cyclotron waves propagation and absorption in a plasma to be simulated in an accurate and numerically efficient fashion. It has been extensively employed, among other studies, to simulate Tore Supra experiments [7]. In order to facilitate its use as a tool for the design and analysis of future experiments in WEST, some further developments have been recently carried out, and are summarized in Figure 1.

The REMA code requires the magnetic equilibrium, plasma parameters and the EC antenna configuration as inputs. Based on general wave and ray-tracing theory, the code provides the toroidal and poloidal projections of the ray trajectories, as well as the power and driven current density profiles and the total fraction of absorbed power. To facilitate its use, REMA has been directly

interfaced with the WEST IMAS database. This has allowed integrated modelling simulations of existing pulses including an additional source of EC power to be performed. It is worth mentioning that the results of these simulations are also written in the IMAS format in preparation of potential further simulations.

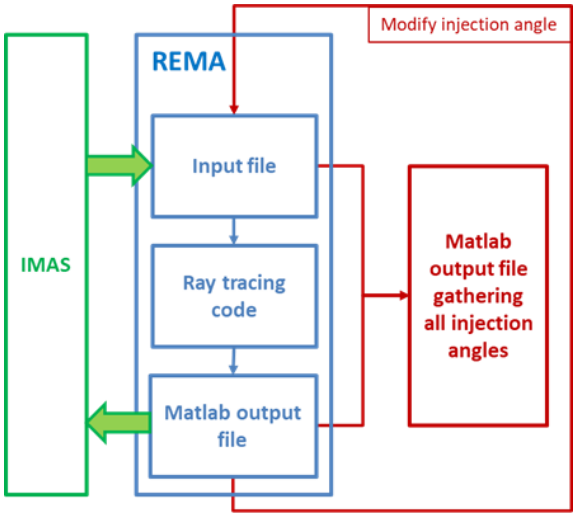

Figure 1: General view of the improvements performed on the REMA code.

The main objective of these developments is the determination of the operational domain for the EC antenna in terms of wave toroidal and poloidal injection angles. For this aim, a dedicated routine has been developed to sweep all mechanically reachable injection angles, and to build a synthetic view of the obtained results. As an illustration, Figure 2 displays the location of the EC absorption (in normalized radius) as a colour map over the whole toroidal/poloidal injection angle grid in the case of WEST shot 55799 [8]. Also shown are contours indicating the total absorbed power fraction. As an example, the outermost contour shows the 70% absorbed fraction in the first pass through the plasma.

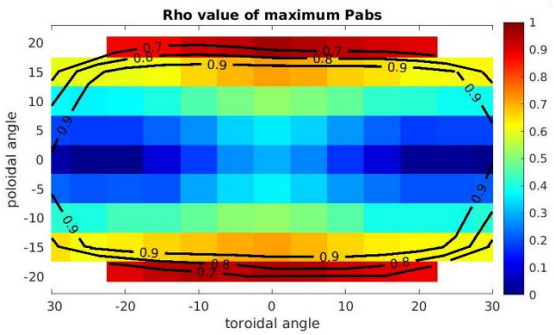

Figure 2: Location of the absorption (in normalized radius depending on the injection angle for WEST shot 55799. The superimposed labeled black contours show the fraction of total absorbed power.

3 Determination of the limits for the new ECRH system

As a preparation for the new ECRH system implementation on WEST, it is necessary to define its operational domain. It characterizes the injection angle limits, beyond which the waves are insufficiently absorbed by the plasma independently of its parameters. This is necessary for device safety, as poor absorption can result in levels of radiofrequency power in the vacuum vessel, potentially dangerous for the various systems installed in WEST.

3.1 Plasma profiles dependence for the wave absorption and propagation

In order to define those limits, the set of plasma conditions for which the operational domain is the widest needs to be identified. Any changes of the plasma parameter with respect to these conditions will be included in the maximum limits. This is why the propagation and absorption behaviour as a function of the plasma parameters needs to be precisely characterized.

As is well known, the electron density has a direct influence on the wave propagation properties. Indeed, larger densities result in larger wave refraction in the plasma, until a cut-off is attained and the wave is completely reflected. In WEST, because the magnetic field is high, the cut-off is expected at a local electron density of $n_{e,limit} \sim 14\times10^{19} m^{-3}$. Considering a typical line-averaged electron density $n_l \sim 6\times10^{19}\ m^{-3}$, cut-off is rarely reached as $n_{e,max}$ is usually lower than $n_{e,limit}$. In order to establish the widest operational domain, appropriate injection angles should be found, that compensate for wave refraction in the case of high-density plasmas.

In Figure 3, it is observed that similar absorption locations (in the vicinity of the resonance layer, shown with a black line) are obtained for different injection angles when the line-averaged density is varied in the range expected in WEST scenarios, i.e. from $n_l \sim 2\times10^{19} m^{-3}$ to $9\times10^{19} m^{-3}$.

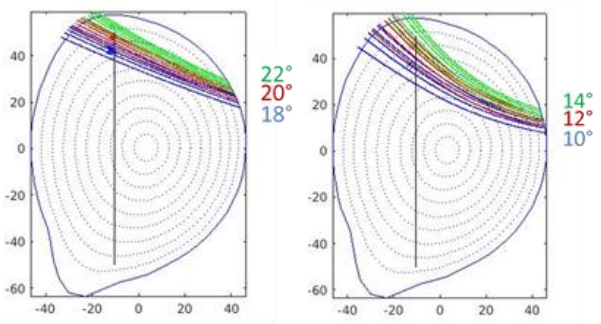

Figure 3: Poloidal projection of the ray trajectories for a line-averaged density of $2\times10^{19}\ m^{-3}$ (left) and $9\times10^{19}\ m^{-3}$ (right). The vertical black line shows the EC resonance layer. The corresponding poloidal injection angles are indicated in the figure.

The modification of the magnetic field has a negligible influence on the wave propagation properties but has a strong influence on the resonance location. Indeed, if the 105 GHz frequency has been chosen in order to get central absorption for the nominal WEST magnetic field and oblique propagation (for current drive applications), decreasing the magnetic field moves the resonance towards the high field side.

Modifying the electron temperature has little influence on the wave propagation. Larger temperatures

are known to increase the absorbed power fraction. On the other hand, close to the plasma edge, waves are generally poorly absorbed by the plasma. Increasing the temperature therefore allows absorption locations closer to the plasma edge to be obtained with a sufficient absorbed fraction, thereby enlarging the operational domain.

As a conclusion, the optimal conditions for which the injection limits are maximised are low density, high temperature and nominal magnetic field. This corresponds in WEST to a line-averaged electron density of around $2\times10^{19}m^{-3}$, an electron temperature around 6keV and a central magnetic field around 3.7T.

3.2 Operational limits determination

With the global plasma conditions now being defined, it is useful to characterize the limits within which EC waves can be absorbed from the core to the edge, for all three steerable mirrors. For the middle mirror, it is possible to restrict the domain to the upper or lower part of the plasma, as they are approximately symmetric, except for the divertor area (see Figure 4).

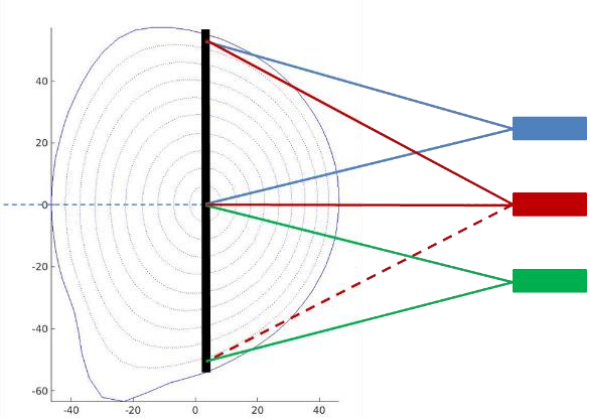

Figure 4: Operational limits determination method for the three steerable mirrors. Only the upper part of the plasma is considered for the middle mirror.

From the REMA simulations consisting of detailed injection angles scans described previously (see Figure 2), a global view of the system capabilities is obtained. Figure 5 shows results for the lower mirror, inside the limits defined by the antenna mirror movements.

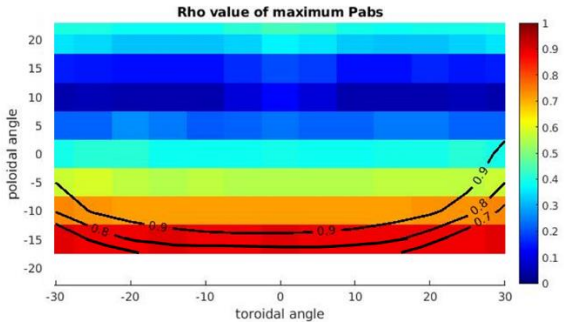

Figure 5: Location of the absorption in terms of normalized radius (colormap) depending on the injection angles for the lower mirror in optimal conditions. Contours define a few values of the absorbed fraction (0.7, 0.8, 0.9).

Repeating the process for the upper and middle mirrors, and refining the limits by running additional ray-tracing simulations, the operational domain, for every mirror has been obtained, as shown in Figure 6.

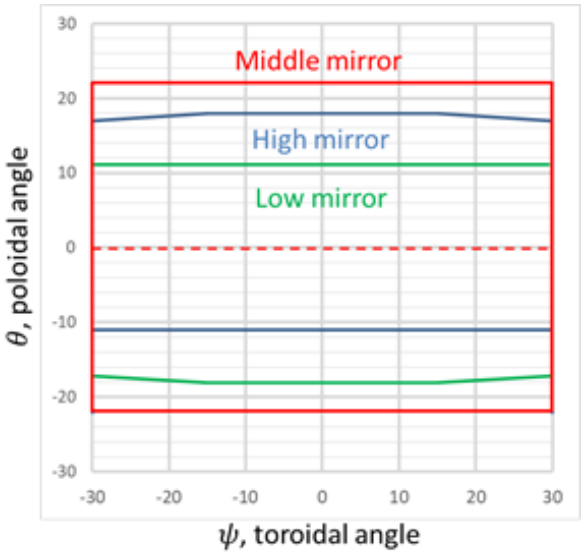

Figure 6: Operational domain for the three steerable mirrors.

3.3 Restricted absorption domain for different plasma conditions

Whereas the previous global studies establish that outside of the determined limit, waves are poorly absorbed, more detailed analyses are needed to better characterize the acceptable injection angles depending on the plasma conditions. A study was started to have a general view over the characterization of satisfying injection angles with respect to absorption properties for the first harmonic. For this purpose, three different plasmas are considered: low-temperature (~1keV at the centre), moderate-temperature with additional heating (~3keV) and high-temperature (~6keV). For these temperatures, the objective is to estimate the magnetic field domain compatible with the ECRH system, i.e. with an acceptable domain of injection angles and a sufficiently wide range of possible absorption locations. Then, simulations have been run at the magnetic field limit for a low-density (n_l~2×10^{19} m^{-3}) and a high-density plasma (n_l~9×10^{19} m^{-3}). The final domain with respect to wave absorption for the three different temperatures has been determined by combining the domains of low and high-density results. Figure 7 allows us to determine some general tendencies.

First observable result that is highly expectable is that higher is the temperature and wider is the domain with acceptable absorption. That way, off-axis injection is restricted as the local temperature is lower than the core one. To maximise the absorption, it seems that a centred poloidal and toroidal injection is preferable.

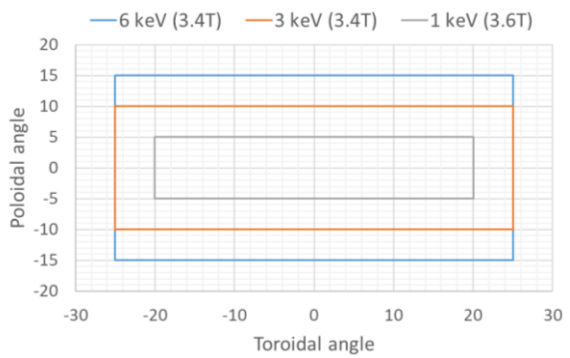

Figure 7: Restricted domain for the middle mirror, depending on electron temperature and central magnetic field.

4 Integrated modelling of WEST scenarios with EC power

The objective of the next study is to evaluate the potential positive impact of EC power in WEST scenarios, and to evaluate its influence compared to the other, already operating, radiofrequency heating systems (LH, in the present case).

4.1 Radiative collapse in WEST

As comprehensively presented in Ref. [9], WEST plasmas with LH power occasionally exhibit temperature collapses due to the power radiated by tungsten impurities in the plasma core exceeding the electron heat source. Shot 55025 displays an example of such a collapse (Figure 8). Around 9.5s, a fast decrease of the electron temperature limited to the central region ($\rho<0.4$) is observed. This coincides with a sudden increase of the tungsten density estimated from bolometry measurements, and a simultaneous decrease of the HXR (Hard X-ray) signal indicating a modification of the LH power deposition [9].

4.2 Impact of the ECRH system

The first study concerns the power deposition profiles. On one hand, the LH deposition profile has been simulated with a reduced model included in the METIS code [10]. The plasma kinetic profiles used have been fitted from experimental measurements. On the other hand, REMA has been run with adapted injection angles in order to obtain a centrally localized absorption in the conditions of WEST shot 55025. Figure 9 illustrates the differences between the computed LH and EC power deposition profiles.

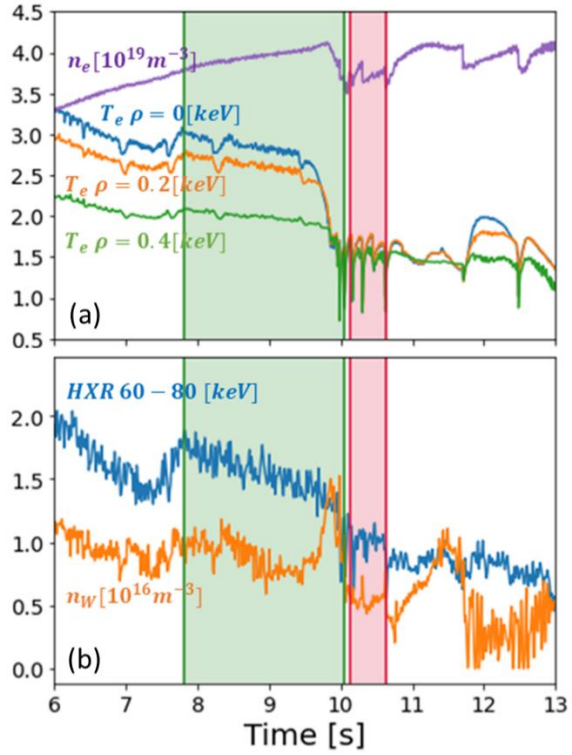

Figure 8: WEST shot 55025. (a) Electron temperature at different radial locations, line-averaged electron density; (b) HXR emission in the energy band 60-80 keV and estimated central tungsten density (adapted from Ref. [9]).

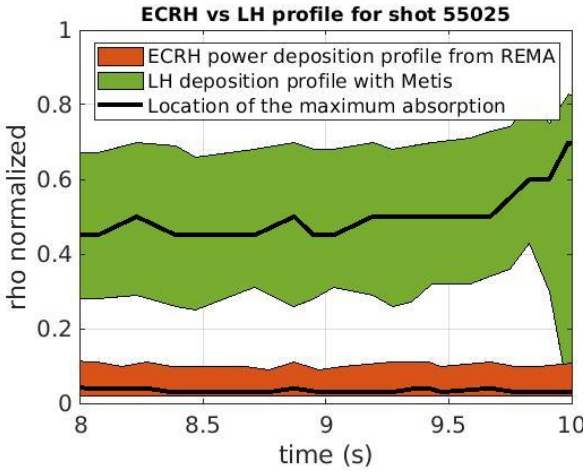

Figure 9: Evolution of LH and EC power deposition profiles in shot 55025 (colored areas: full width at half maximum of the deposition; black line: location of deposition maximum)

Firstly, typical LH deposition profiles, in the multi-pass regime typical of WEST, are radially wider radially than ECRH profiles. In addition, whereas ECRH allows power to be deposited in the core, the maximum of LH deposition is more off-axis. The second observation that makes ECRH interesting is the invariance of the deposition profiles with respect to the electron temperature decrease. When the collapse, characterized by a fast temperature decrease at t~9.5, occurs, the LH deposition moves more and more off-axis and the maximum location reaches ρ~0.7 at t~10s, thereby reducing the heat source on electrons. In comparison, the EC deposition profile is not affected. Its width and maximum remain constant, which allows efficient

electron heating in the core to be maintained even in the presence of a radiated power increase caused by impurities.

Integrated simulations using the RAPTOR transport code [6] have been performed in order to further assess the benefits of an EC power source in WEST scenarios. This code allows the evolution of the electron temperature depending on turbulent transport and heat source to be simulated. For the present simulations, the Bohm-Gyrobohm [11] transport model has been used. In order to compare the electron temperature evolution with LH and EC power, shot 55025 has been considered, at time t=8s, i.e. during the flat-top phase of the discharge. If most of the data was taken from experiment and diagnostics, METIS interpretative shot allowed to fill the missing data. First simulations have been run using the METIS output IMAS datafile and varying the W concentration from 0 to 5×10^{-4}. Secondly, LH power (2.8MW) has been replaced by a central source of EC power, varied between 0 and 3MW and W concentration has also been varied. Resulting central electron temperature has been determined and is therefore displayed as a colour map in Figure 10.

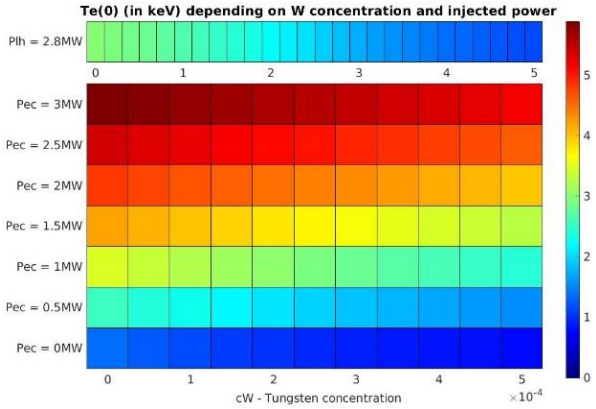

Figure 10: Central electron temperature as a colour map depending on the injected power and the tungsten concentration.

Firstly, for approximately equivalent injected power levels (2.8 MW for LH and 3MW for ECRH), it is observed that the electron temperature in the core gets twice higher with ECRH for low tungsten concentrations. At higher tungsten concentrations, it becomes around five times larger. The second quantitative observation is that the same electron temperature is obtained for EC power lever four times lower than the LH power level when the tungsten concentration is low. The difference is even larger for higher tungsten concentration. In terms of core electron heating, ECRH is therefore more efficient due to its more central deposition profile. This observation is not surprising, as the main role of LH waves in WEST is efficient current drive rather than central electron heating. ECRH, in principle, should prevent a radiative collapse at the levels of tungsten concentrations observed in some situations from occurring. These first studies therefore demonstrate the major benefit that can be anticipated from the future EC system in WEST.

5 Prospects

Additional integrated modelling simulations are now ongoing using RAPTOR, to better characterize the impact of the central heating and current drive from EC waves. The next objectives are to run refined simulations using the neural network-based transport model associated to the quasilinear gyrokinetic code QuaLiKiz (QLKNN) for turbulent transport [12] and LUKE to have a first principle based modelling of the LH deposition profiles [13]. Then, time-evolving integrated modelling of discharges exhibiting increasing of the core tungsten density in the presence of EC power will be performed. These simulations will be applied to a wide range of shots from the WEST database. Finally, in the future, the capabilities of the new ECRH/ECCD system to control MHD effects during the ramp-up and plateau phases in WEST plasmas will be studied.

Acknowledgements

This work is the result of a collaboration with many workers at IRFM, most notably the ECRH team, and I would like to thank them all for their help and support.

References

1. R.J. Dumont et al., Plasma Phys. Control. Fusion **56,** 075020 (2014).
2. J. Bucalossi et al., Nucl. Fusion **62**, 042007 (2022).
3. L. Delpech et al., this conference (2022).
4. V. Krivenski et al., Nucl. Fusion **25**, 127 (1985).
5. C. Angioni et al., Nucl. Fusion **57** 056015 (2017).
6. F. Felici and O. Sauter, Plasma Phys. Control. Fusion **54** 025002 (2012).
7. M. Goniche et al., Proc. 47th EPS Conference on Plasma Physics (2021).
8. M. Lennholm et al., Nucl. Fusion **43** 1458 (2003).
9. V. Ostuni et al., Nucl. Fusion **62** 106034 (2022).
10. J.F. Artaud et al., Nucl. Fusion **58**, 105001 (2018).
11. M. Erba, et al., Plasma Phys. Control. Fusion **39**, 261 (1997).
12. K.L. van de Plassche et al., Phys. Plasmas **27**, 022310 (2020).
13. Y. Peysson and J. Decker, Fusion Science and Technology **65** 22 (2014).